Supporting Information

Kang et al. 10.1073/pnas.1113865109

SI Materials and Methods

Mouse Strains. Receptor for advanced glycation endproducts (RAGE) KO (*Rage*$^{-/-}$) mice (SVEV129 × C57BL/6) were a kind gift from Angelica Bierhaus (University of Heidelberg, Heidelberg, Germany) (1). *Pdx1-Cre* and *Kras*$^{G12D/+}$ transgenic mice on the C57BL/6 background were received from Mouse Models of Human Cancers Consortium/National Cancer Institute Mouse Repository. The genotypes *Pdx1-Cre*:*Kras*$^{G12D/+}$ (KC) and *Rage*$^{-/-}$ were crossed to generate conditional-mutant mice *Pdx1-Cre*:*Kras*$^{G12D/+}$:*Rage*$^{-/-}$ (KCR). Genotyping was done by standard PCR. Pancreas tissues was collected from age- and sex-matched KC and KCR mice at several different time points and fixed immediately in 10% neutral buffered formalin, then paraffinized and stained with H&E in the standard fashion. At least four nonserial pancreatic sections were graded for dysplastic ducts by an independent pathologist with special expertise in pancreatic cancer who was blinded to mouse genotype. Number of low- and high-grade dysplastic ducts was normalized to the number of total ducts present in the specimen and expressed as a percentage of total ducts. The scores for the quality of sample and quantity of each stain were normalized.

Cell Proliferation and Colony-Formation Assay. Cell proliferation was evaluated by using the Cell Counting Kit-8 (Dojindo Laboratories) according to the manufacturer's instructions. Cell Counting Kit-8 uses the highly water-soluble tetrazolium salt 2-(2-methoxy-4-nitrophenyl)-3-(4-nitrophenyl)-5-(2,4-disulfophenyl)-2H-tetrazolium, monosodium salt (WST-8), which has a detection sensitivity that is higher than other tetrazolium salts such as 3-[4,5-dimethylthiazol-2-yl]-2,5-diphenyltetrazolium bromide (MTT). Colony-formation assay was performed as previously described (2).

Gene Transfection and shRNA. Autophagy protein 5 (ATG5) shRNA and RAGE shRNA (Sigma) or pcDNA3-Stat3 expression vector (Addgene) or pUNO1-RAGE (InvivoGen) were transfected into cells with Lipofectamine 2000 (Life Technologies) according to the manufacturer's instructions. Stable RAGE shRNA-expressing pancreatic cancer cells were generation as previously described (3).

Western Blotting. Immunoblotting was performed by lysing cell samples, electrophoresing on 4–12% (wt/vol) Criterion XT Bis-Tris gels (Bio-Rad), incubating with primary antibodies overnight at 4 °C, and detecting primary antibodies with HRP-conjugated secondary antibody (Cell Signaling Technology) and enhanced chemiluminescence (Pierce) as described (3). The relative band intensities were quantified by using Gel-Pro Analyzer software (Media Cybernetics) and normalizing to the loading control.

Immunohistochemistry and Immunofluorescence. Tissues were embedded in optimum cutting temperature cryomedium (Sakura) and cut into 8-μm sections as described previously (3). Sections were subjected to immunohistochemical and immunofluorescent staining as described in ref. 4. For immunofluorescence, tissue sections were stained with microtubule-associated protein light chain 3 (LC3), Ki67 or STAT3, and phosphorylated STAT3 (p-STAT3) antibodies, followed by Alexa Fluor 488- or Cy3-conjugated secondary antibodies. Nuclear morphology was analyzed with the fluorescent dye Hoechst 33342 (Invitrogen). Mitochondria was analyzed with anti-complex I subunit GRIM-19 (MitoSciences). TUNEL assay was performed with the In Situ Cell Death Detection Kit, according to the manufacturer's instructions (Roche).

Autophagy Assays. Autophagic flux was measured by Western blotting or imaging for LC3 with or without inhibitors of early [e.g., 3-methyladenine (3-MA)] and late [e.g., bafilomycin A1 (Baf-A1)] autophagy as previously described (5). Images were collected with a laser-scanning confocal microscope (FluoView FV1000; Olympus) using a 60× Plan Apo/1.45 oil-immersion objective and FluoView software (FV10-ASW 1.6; Olympus). Images were acquired digitally from a randomly selected pool of 5–10 fields under each condition. Transmission electron microscopy (TEM) assessment of autophagic vacuoles or organelles was performed as previously described (6). ATG12–ATG5 complexes were assayed by using a specific ATG5 antibody that recognized ATG5–ATG12 conjugated form (~55 kDa) and free ATG5 (~30 kDa).

ATP Assay. The ATP content in whole-cell or tissue extracts was determined with a luminescent ATP detection kit (ATPlite; PerkinElmer Life Sciences) according to the manufacturer's instructions. The luminescent intensity was measured with a microplate reader (Synergy 2; BioTek Instruments). In parallel, cell number in whole-cell samples and protein concentration in the tissue extracts were conventionally determined by trypan blue exclusion or bicinchoninic acid assay, respectively. The results in cells are expressed as relative ATP level compared with controls after normalizing for cell number. The results in tissues are expressed as relative ATP level compared with controls after normalizing for protein concentration.

Complexes I and IV Enzyme Activity Assay. The activity of complexes I and IV was determined with the Enzyme Activity Assay Kit (MitoSciences) according to the manufacturer's instructions. The enzyme activity of the control group was set as 100%.

Statistical Analysis. Data are expressed as means ± SD of three independent experiments performed in triplicate. One-way ANOVA was used for comparison among the different groups. When the ANOVA was significant, post hoc testing of differences between groups was performed by using a least significant difference test. $P < 0.05$ was considered significant.

1. Liliensiek B, et al. (2004) Receptor for advanced glycation end products (RAGE) regulates sepsis but not the adaptive immune response. *J Clin Invest* 113:1641–1650.
2. Tang D, et al. (2010) HMGB1 release and redox regulates autophagy and apoptosis in cancer cells. *Oncogene* 29:5299–5310.
3. Kang R, et al. (2010) The receptor for advanced glycation end products (RAGE) sustains autophagy and limits apoptosis, promoting pancreatic tumor cell survival. *Cell Death Differ* 17:666–676.
4. Kojima K, et al. (2007) Inactivation of Smad4 accelerates Kras^{G12D}-mediated pancreatic neoplasia. *Cancer Res* 67:8121–8130.
5. Mizushima N, Yoshimori T, Levine B (2010) Methods in mammalian autophagy research. *Cell* 140:313–326.
6. Tang D, et al. (2010) Endogenous HMGB1 regulates autophagy. *J Cell Biol* 190:881–892.

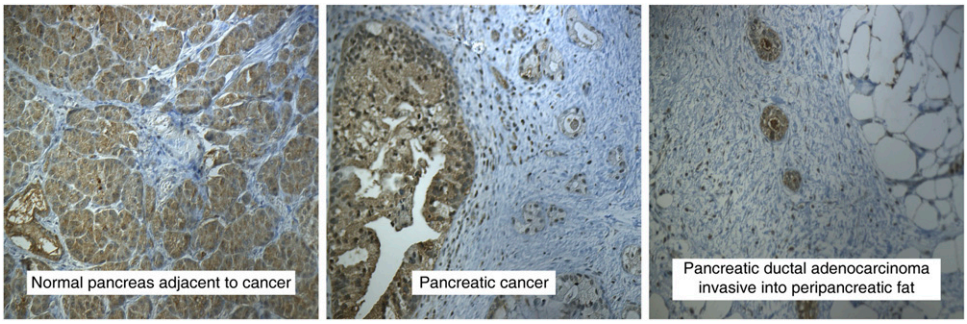

Fig. S1. Immunohistochemical demonstration of RAGE expression in human pancreatic cancer specimens.

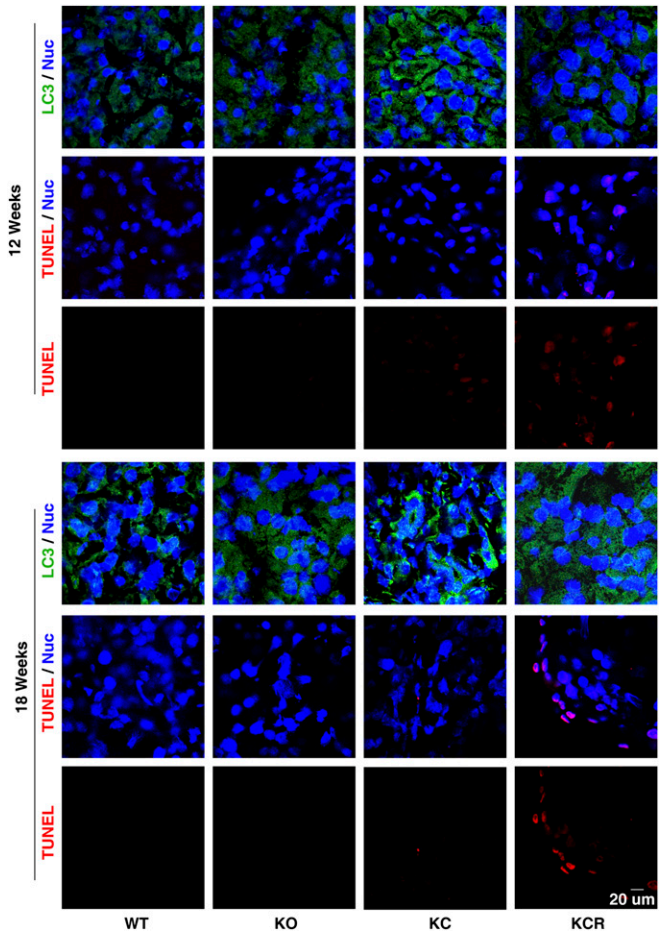

Fig. S2. Enhanced autophagy and apoptosis at 12 and 18 wk in the pancreas of KC mice.

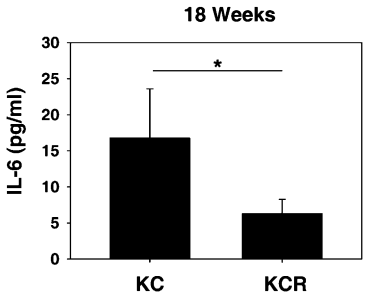

Fig. S3. Serum IL-6 levels are elevated in KC and diminished in KCR mice (n = 3 animals per group; *$P < 0.05$).